

## Surface Wind and Stress

WT Liu, California Institute of Technology, Pasadena, CA, USA

© 2015 Elsevier Ltd. All rights reserved.

### Synopsis

The basics of scatterometry and air–sea turbulence transfer are discussed to bring out the capabilities of space sensors in measuring ocean surface stress and wind vectors. The scientific significance of wind and stress are described. Past knowledge of stress characteristics was based on those of wind, because of the lack of stress measurements. Using the unique measurement of stress by the scatterometer, the differences between stress and wind over oceanfronts and in hurricanes are revealed. Wind speed retrieval from measurements of radar altimeter, microwave radiometer, and synthetic aperture radar is summarized. Potential improvements in measuring wind and stress are suggested.

### Introduction

Wind is air in motion, and it is a vector quantity with a magnitude (speed) and a direction. Sailors understand both the importance and the difficulty in getting information on wind over oceans. Textbooks still describe global ocean wind distribution in sailors' terms: the calms of the doldrums and horse latitudes, the steady trade winds, and the ferocity of the roaring forties. These features are clearly visible in [Figure 1](#), which is derived from one day of observations by a space-based scatterometer, QuikSCAT. Just a few decades ago, almost all ocean wind measurements came from merchant ships. However, the quality and geographical distribution of these wind reports were uneven. Today, operational numerical weather prediction (NWP) also gives us wind information, but NWP depends on models, which are limited by our knowledge of the physical processes and the availability of data.

The ocean interacts with the atmosphere in nonlinear ways; processes at one scale affect processes at other scales. Adequate wind coverage could be achieved only from the vantage point of space. Space-based microwave radars measure ocean surface roughness day and night, under clear and cloudy conditions. Ocean surface roughness is driven by stress, the turbulent transfer of momentum between the ocean and the atmosphere. Stress is another vector quantity closely related to wind. The microwave scatterometer is the best-established instrument to measure surface stress magnitude and direction, and has been promoted as a wind sensor. The scientific significance of wind and stress is introduced in the Scientific Significance section. The principles of the scatterometer are summarized in the Scatterometry section.

The primary functions of the radar altimeter, the synthetic aperture radar (SAR), and the microwave radiometer are not wind measurement, but they give wind speed as a secondary product. Wind speed, even without direction, is important, and wind speed from these sensors can be applied with directional information derived from other means. The space-based polarimetric radiometer also shows sensitivity to wind direction under favorable conditions. These instruments are described in the Other Sensors section.

While the general public knows and feels the wind, very few people know what stress is. Even for oceanographers, the concept of stress distribution is largely derived from that of wind, because there was no large-scale measurement of stress

over the ocean until the launch of the first scatterometer. The relation and the difference between wind and stress are discussed in the Relations between Wind and Stress section. Potential improvements in space-based measurements of wind and stress are given in the Potential Improvements and Conclusion section.

### Scientific Significance

Ocean wind is strongly needed for marine weather forecasting and to avoid shipping hazards. Surface wind convergence brings moisture and latent heat that drive deep convection and fuel marine storms. The significance of wind measurement is clearly felt, for example, when a hurricane suddenly intensifies and changes course, or when the unexpected delay of monsoon brings drought. Detailed distribution of wind power is also needed for the optimal deployment of floating wind farms on the open sea that are enabled by new technology.

For oceanographers, it is stress more than wind that drives ocean circulation. The two-dimensional stress field is needed to compute the divergence and curl (vorticity) that control the vertical mixing. The mixing brings short-term momentum and heat trapped in the surface mixed layer into the deep ocean, where they are stored over time. It also brings nutrients and carbon stored in the deep ocean to the surface, where there is sufficient light for photosynthesis. The horizontal currents, driven in part by stress, distribute the stored heat and carbon in the ocean. Stress affects the turbulent transfer of heat, moisture, and gases between the ocean and the atmosphere and is critical in understanding and predicting weather and climate changes.

### Scatterometry

During the Second World War, marine radar operators observed noises on their radar screens, which obscured small boats and low-flying aircraft. They termed this noise 'sea clutter'. This clutter was the backscatter of the radar pulses by the small waves on the ocean's surface. The radar operators at that time were quite annoyed by these noises, not knowing that, a few decades later, scientists would make important applications with them.

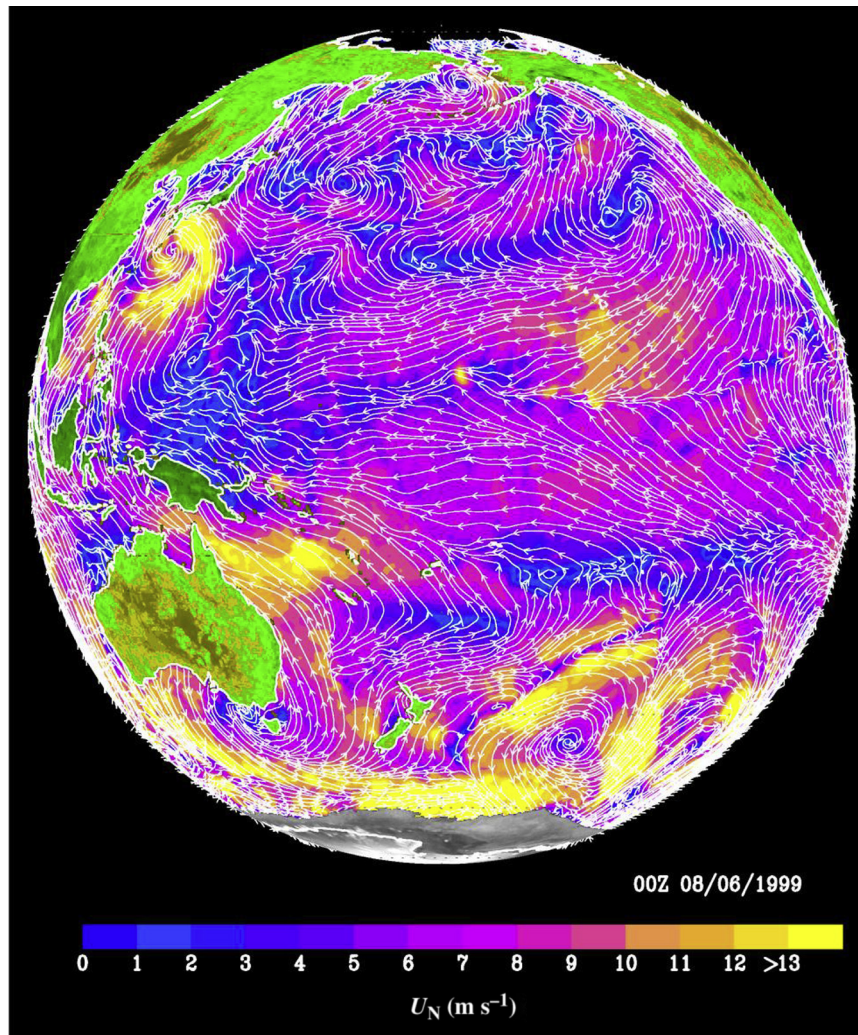


**Figure 1** Over the ocean, white streamlines indicating wind direction are superimposed on the color image of  $U_N$  at 00Z on 6 August 1999, derived from objective interpolation of the observations by QuikSCAT. Normalized backscatter coefficients measured by the same instrument over land and Antarctica are also displayed.

The scatterometer sends microwave pulses to the Earth's surface and measures the power backscattered from the surface roughness. The roughness may describe the characteristics of polar ice or vegetation over land. Over the ocean, which covers nearly three-quarters of the earth's surface, the surface roughness is largely due to the small centimeter waves on the surface. These surface waves are believed to be in equilibrium with the local stress. The backscatter depends on not only the magnitude of the stress but also the stress direction relative to the direction of the radar beam (azimuth angle). The capability of measuring both stress magnitude and direction is the major unique characteristic of the scatterometer.

At incident angles greater than  $20^\circ$ , the radar return is governed by Bragg scattering, and the backscatter increases with stress. The backscatter is governed by the in-phase reflections from surface waves. The geophysical model functions (GMF), from which ocean surface wind and stress are retrieved from the observed backscatter, in the form of the normalized radar cross-section ( $\sigma_o$ ), are largely based on empirical fits of

data. The symmetry of backscatter with wind direction requires observations at many azimuth angles to resolve the directional ambiguity. Because of uncertainties in the wind retrieval algorithm and noise in the backscatter measurements, the problem of directional ambiguity was not entirely eliminated even with three azimuthal looks in the scatterometers launched after SEASAT (in 1978). A median filter iteration technique has been commonly used to remove the directional ambiguity.

Because there is much more wind information than stress information and the public is more familiar with wind than stress, an equivalent neutral wind ( $U_N$ ) is used as the geophysical product of the scatterometer. By definition,  $U_N$  is uniquely related to stress, while the relation between stress and the actual wind depends on atmospheric stability (see [Relations between Wind and Stress](#) section). Although scatterometers have been known to measure surface stress, they have been used and promoted as wind-measuring instruments, and  $U_N$  has been used as the actual wind, particularly in operational

weather applications. More explanation is given in the Relations between Wind and Stress section.

Over the large expanse of ocean, which is quasi-stationary and horizontally homogeneous under near-neutral conditions, and where ocean surface current is negligible,  $U_N$  may be the same as the actual wind. Over the sharp horizontal current shear and temperature gradients of oceanfronts, however, stress variation could be very different from that of winds. The observation of the rotation of scatterometer measurement in opposition to the surface current, in the meanders of the Kuroshio Extension current, is a clear characteristic of turbulent stress generated by shear. One would expect wind to be dragged in the same direction as the current, but stress is the vector difference between wind and current, and the direction would be deflected from the current. Figure 2 clearly shows that where the vorticity of  $U_N$  measured by QuikSCAT is positive, the vorticity of the surface current measured by the drifters is negative and vice versa, indicating opposite rotations.

The ubiquitous spatial coherence between sea surface temperature ( $T_s$ ) and  $U_N$ , measured by the scatterometer and

found under a variety of atmospheric conditions, is also characteristic of turbulent stress generated by buoyancy. In the unstable region, atmospheric buoyancy generates turbulent momentum transport and increases the stress magnitude. Figure 3(a) shows the coherence over the Kuroshio Extension. Figure 3(b) shows similar coherence between  $T_s$  and  $U_N$  computed from a uniform wind field under similar stability conditions, demonstrating that the coherence is a characteristic of stress and not wind. Factors affecting larger-scale wind, such as the pressure gradient force, the Coriolis force, and baroclinicity, are not important at the small scales of turbulence, and that is the reason for ubiquitous coherence. The higher stress over warmer water affects atmospheric wind aloft, but the influence will be subjected to these large-scale factors. Ocean parameters, such as surface current and temperature, are needed to derive wind from stress in these frontal regions.

Retrieving strong winds from the scatterometer is also difficult. The problem is obvious in Figure 4, which is derived from NASA's scatterometer on QuikSCAT measuring at the Ku-band (14 GHz). Data for the 12 hurricanes in the North

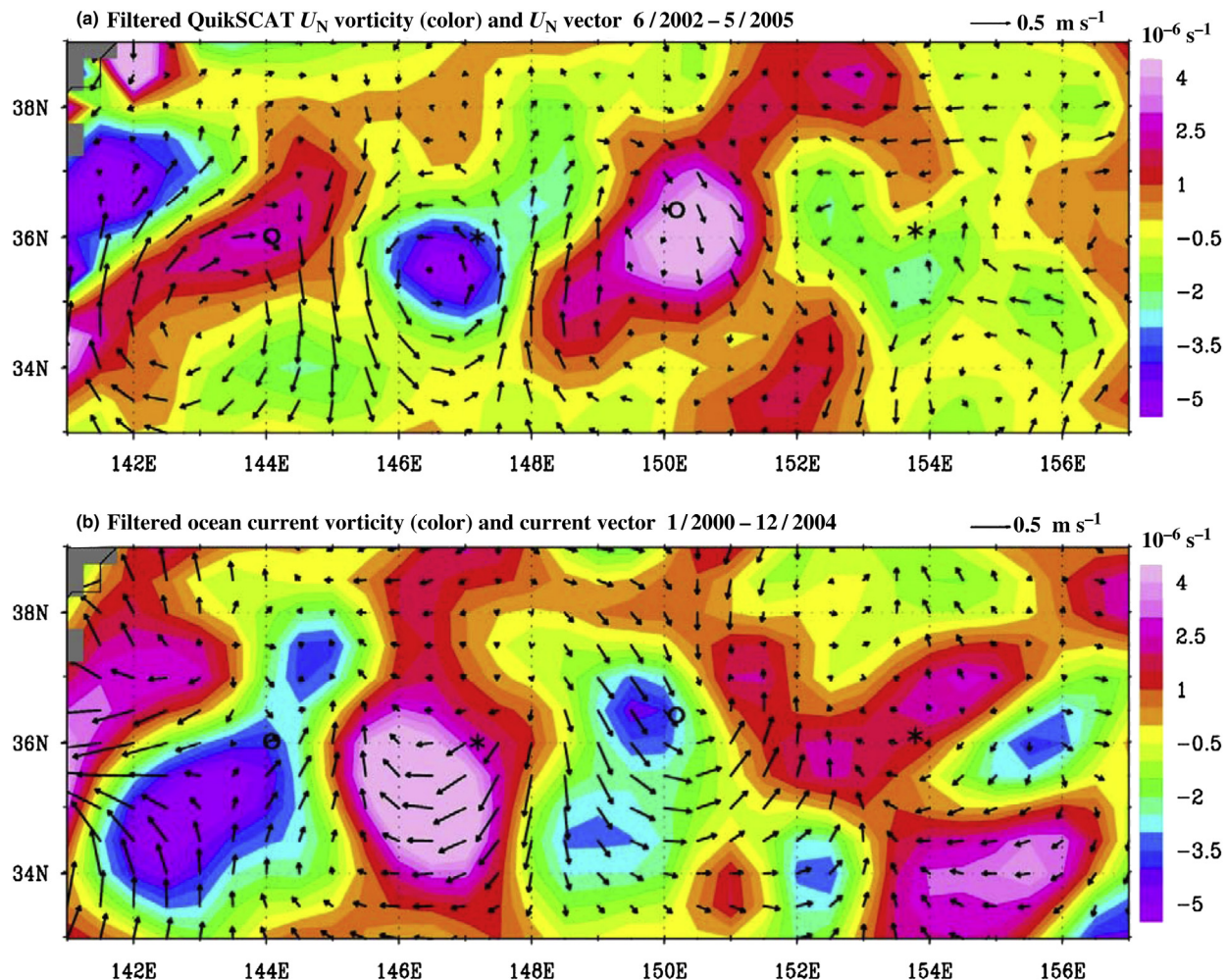


**Figure 2** (a) Filtered vector (black arrows) superimposed on vorticity (color,  $10^{-6} \text{ s}^{-1}$ ) of  $U_N$  observed by QuikSCAT, averaged from June 2002 to May 2005. (b) Filtered vector (black arrows) superimposed on vorticity (color,  $10^{-6} \text{ s}^{-1}$ ) of the surface current measured by Lagrangian drifters, averaged from 2000 to 2004. The large-scale gradients are removed by a two-dimensional filter.

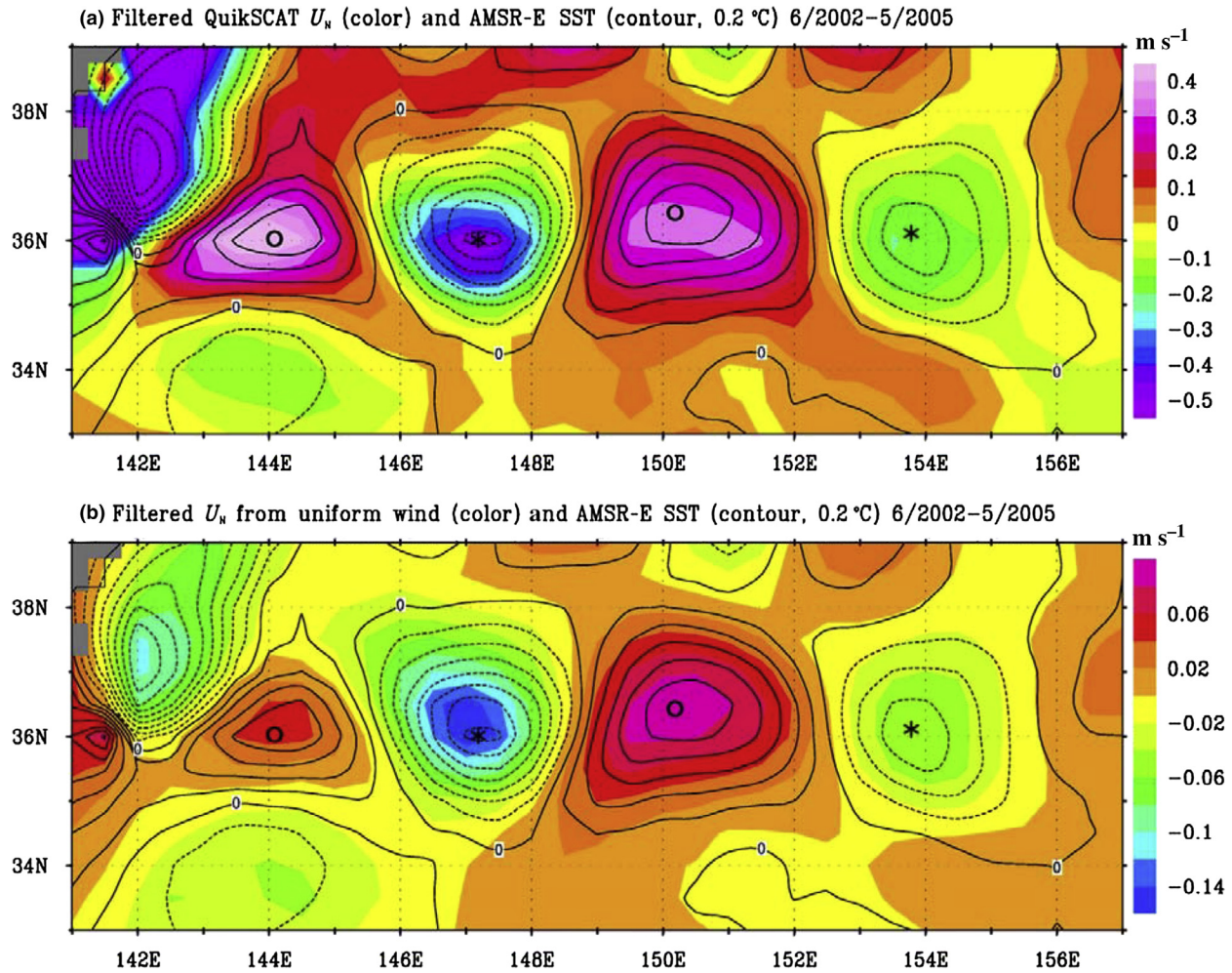


**Figure 3** (a) Isotherms of filtered  $T_s$  measured by the Advanced Microwave Scanning Radiometer for EOS (AMSR-E; EOS is NASA's Earth Observing System) ( $0.2^\circ\text{C}$  interval) superimposed on (a) filtered magnitude of QuikSCAT  $U_N$  (color,  $\text{m s}^{-1}$ ); and (b) filtered  $U_N$  computed from a uniform wind field of  $u = 7.5 \text{ m s}^{-1}$  (color,  $\text{m s}^{-1}$ ), averaged from June 2002 to May 2005. Solid and broken lines represent positive and negative values, respectively. The same filter as in Figure 2 is applied.

Atlantic in the 2005 season, excluding those with over 10% chances of rain, were examined. Figure 4 shows that, in moderate winds ( $U < 35 \text{ m s}^{-1}$ ), the logarithm of  $\sigma_o$  (in db) increases linearly with the logarithm of wind speed at both polarizations. At strong winds ( $U > 35 \text{ m s}^{-1}$ ), however,  $\sigma_o$  increases at a much slower rate with increasing wind speed. Similar saturation is found in the European Advanced Scatterometer (ASCAT), measuring at the C-band (5 GHz). Such high wind saturation has also been observed from aircraft flying over hurricanes.

When the model function developed over the moderate wind range is applied to the strong winds, an underestimation of wind speed results. Strong efforts have been made to adjust the model function (slope in Figure 4) in strong winds and to find the right channel (a combination of polarization, frequency, and incident angle) that would be sensitive to the increase of strong winds. The success would be difficult if flow separation occurs at high winds and the surface roughness and stress do not increase with winds, as discussed in the Relations between Wind and Stress section.

## Other Sensors

Both the microwave altimeter and SAR are similar to the scatterometer in the sense that they are active sensors that send microwave pulses to the Earth's surface and measure the backscattered power. The microwave radiometer is a passive sensor, observing the radiance from the Earth and its atmosphere.

While the scatterometer views at oblique angles, the altimeter views at nadir (very small incident angles). At nadir, the backscattered energy is a result of specular reflection (the wavelets serve as small mirrors), and the backscatter is not sensitive to the  $U_N$  direction. Because the instrument is not scanning, data are available only at very narrow (2 km) repeated ground tracks. The coverage of all the past altimeters is poor compared with the scatterometer and the microwave radiometers.

A SAR looks perpendicular to the aircraft path at only one azimuth angle, and cannot resolve the  $U_N$  direction like the scatterometer. SAR has spatial resolutions that are much better

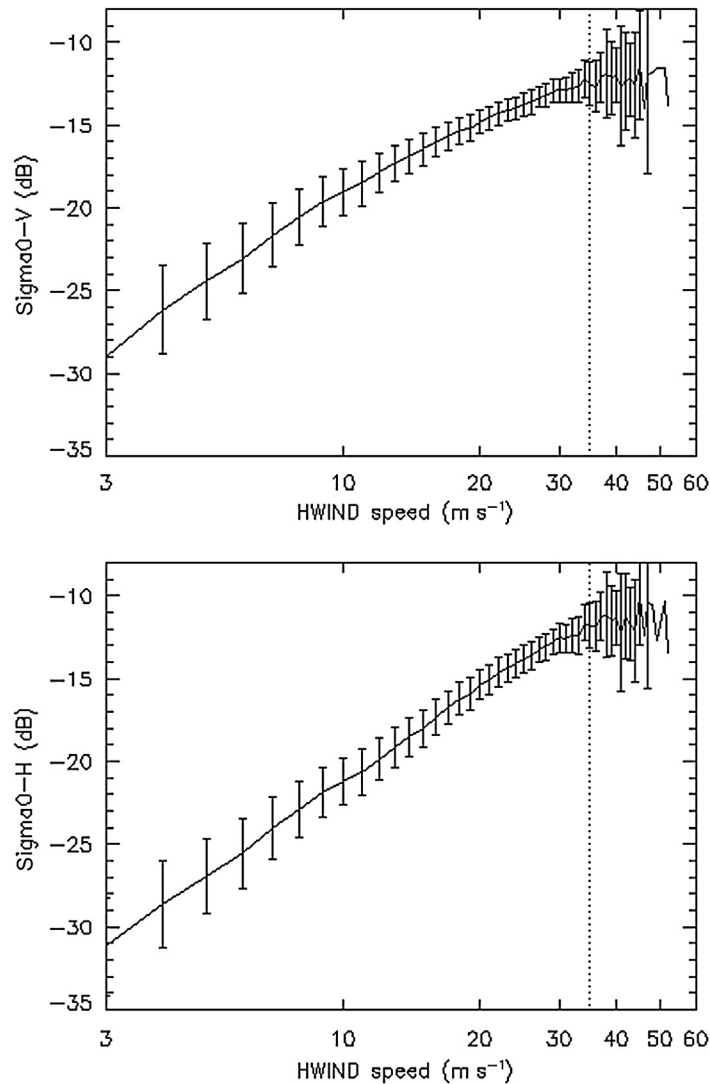


**Figure 4** Normalized radar cross-section at two polarizations measured by QuikSCAT for 12 hurricanes as a function of collocated surface wind provided by the National Hurricane Center.

than those of scatterometers, but the high resolution also introduces higher uncertainties in accuracy caused by secondary effects that affect surface roughness. The instrument and the data-processing procedure are much more complicated than those of the scatterometer, and there have been serious calibration problems. The scatterometer GMF can be used to relate the  $\sigma_o$  measured by SAR to  $U_N$ . However, a particular value of  $\sigma_o$  may correspond to a range of  $U_N$ , depending on the azimuth angle. Hence, in order to retrieve  $U_N$  with the GMF, the  $U_N$  direction must first be specified. Whether the a priori direction information is derived from the orientation of kilometer-scale structure in the SAR image, or from operational NWP models, the spatial scales are much coarser than  $\sigma_o$ .

Ocean surface wind speed has also been derived from the radiance observed by a microwave radiometer. It is generally believed that wind speed affects the surface emissivity indirectly through the generation of ocean waves and foam. Radiometers are designed to observe how the ocean surface operates

primarily at window frequencies, where atmospheric absorption is low. Radiances at frequencies sensitive to sea surface temperature, atmospheric water vapor, and liquid water are also measured; they are used to correct for the slight interference by the atmosphere. It was demonstrated in several airborne experiments that the polarization properties of the sea surface emission vary not only as a function of the wind speed, but also as a function of wind direction. Wind direction-measuring capability has been evaluated for a polarimetric radiometer, WindSat, launched by the US Navy.

### Relations between Wind and Stress

Ocean surface stress ( $\tau$ ) is the turbulent transfer of momentum generated by atmospheric instability caused by both wind shear (difference between wind and current) and buoyancy (vertical density stratification resulting from temperature and

humidity gradients). Direct  $\tau$  measurement has been done in only a few field campaigns in the past. For all practical purposes, our knowledge of  $\tau$  is derived from winds ( $U$ ) at a reference height through a drag coefficient  $C_D$ , which is defined by

$$\tau = \rho C_D (U - U_s)^2 \quad [1]$$

where  $U_s$  is the surface current and  $\rho$  is the air density.

The drag coefficient  $C_D$  has been derived largely in field campaigns. **Figure 5** illustrates the behavior of  $C_D$  at neutral stability. At low wind speed ( $U < 3 \text{ m s}^{-1}$ ), the flow is smooth;  $C_D$  increases with decreasing wind speed. And at moderate wind  $3 < U < 20 \text{ m s}^{-1}$ ,  $C_D$  is an increasing function of wind speed for a rough sea with open fetch. Secondary factors, such as sea states and spray from breaking waves, whose data are not generally available, are not included in this parameterization scheme and should be part of the errors.

In a similar fashion, the turbulent fluxes of heat  $H$  and moisture  $E$  have been related to the mean parameters – wind speed  $U$ , potential temperature  $T$ , specific humidity  $Q$  at 10 m, sea surface temperature  $T_s$ , and the interfacial humidity  $Q_s$  (usually taken to be the saturation humidity at  $T_s$ ), which are the measurements generally available from routine ship reports, through

$$H = \rho c_p C_H (T - T_s)(U - U_s) \quad [2]$$

$$E = \rho C_E (Q - Q_s)(U - U_s) \quad [3]$$

where  $c_p$  is the isobaric specific heat.

In the past, the transfer coefficients,  $C_H$  and  $C_E$ , were approximated with the same values as  $C_D$ . W.T. Liu first postulated in 1979 that, in a rough sea, under a moderate range of winds ( $5\text{--}20 \text{ m s}^{-1}$ ),  $C_H$  and  $C_E$  do not increase with wind speed because of molecular constraint at the interface, while  $C_D$  may still increase because momentum is transported by form drag. Liu's hypothesis, as illustrated in **Figure 5**, was subsequently supported by measurements in field experiments. K. Emanuel argued in 1995, from theoretical and numerical model results, that Liu's hypothesis could not hold at the strong wind regime of a hurricane. To attain the wind strength of a hurricane, the energy dissipated by drag could not keep increasing while the energy fed by sensible and latent heat does not increase with wind speed. His argument puts limits on the increase of  $C_D$  as a function of wind speed. The postulation of

the level of the increase of  $C_D$  with wind speed at hurricane-scale winds was supported by the results of the laboratory studies and the aircraft experiments. Such flow separation may explain the saturation of scatterometer measurements at wind speeds higher than about  $32 \text{ m s}^{-1}$ , as shown in **Figure 4**.

The drag coefficient, or the bulk parameterization of stress, can be expressed as the nondimensional flux–profile relation (also called the similarity function) in the constant flux layer.

$$\frac{U - U_s}{U_*} = 2.5 \left( \ln \frac{z}{z_0} - \psi_U \right) = \frac{1}{\sqrt{C_D}} \quad [4]$$

where  $U_* = (\tau/\rho)^{1/2}$  is the frictional velocity,  $z_0$  is the roughness length, and  $\psi_U$  is a function of the stability parameter, which is the ratio of buoyancy to shear production of turbulence. Typical wind profiles at various stabilities are shown in **Figure 6**. From the zero intercept and the slope of the logarithm profile,  $z_0$  and  $U_*$  can be determined. In general oceanographic applications, the surface current is assumed to be small compared with wind and the atmosphere is assumed to be nearly neutral. Neglecting  $U_s$  and  $\psi_U$  in eqn [4],  $U$  becomes  $U_N$ , and it is uniquely related to  $U_*$  (or  $\tau$ ). To compute  $U_N$  from conventional wind measurements of  $U$  (A on the blue curve in **Figure 6**),  $U_*$  and  $z_0$  are computed as the slope and intercept at the surface of the curve in **Figure 6**. The neutral relation (straight line) defined by  $U_*$  and  $z_0$  will give  $U_N$  (point B). This method has been used in the development and calibration of all scatterometers launched by NASA. At a given level,  $U_N$  is greater than the actual wind ( $U$ ) under unstable conditions but lower under stable conditions. From eqn [4],  $U_N - U = 2.5 U_* \psi_U$ , assuming  $z_0$  depends much stronger on wind shear than buoyancy and this difference is the inherent error of using scatterometer measurements as the actual wind. The formulation of  $\psi_U$  was largely based on experiment data on land, validated with only a small amount of measurement over ocean, and may have considerable uncertainties.

## Potential Improvements and Conclusion

Historically, the European Space Agency used the C-band (5 GHz), but NASA prefers the Ku-band (14 GHz) in their scatterometers. The backscatter at higher frequencies is more sensitive to shorter ocean waves. The Ku-band is more sensitive

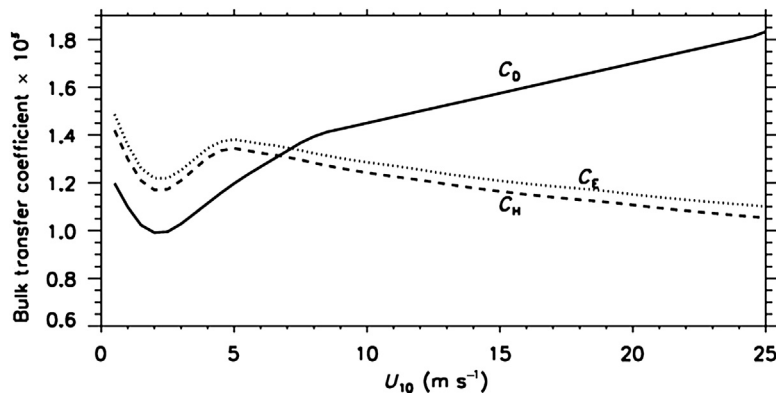


**Figure 5** Variation of the bulk transfer coefficients of momentum (drag coefficient), heat, and moisture with wind speed by Liu et al. (1979).

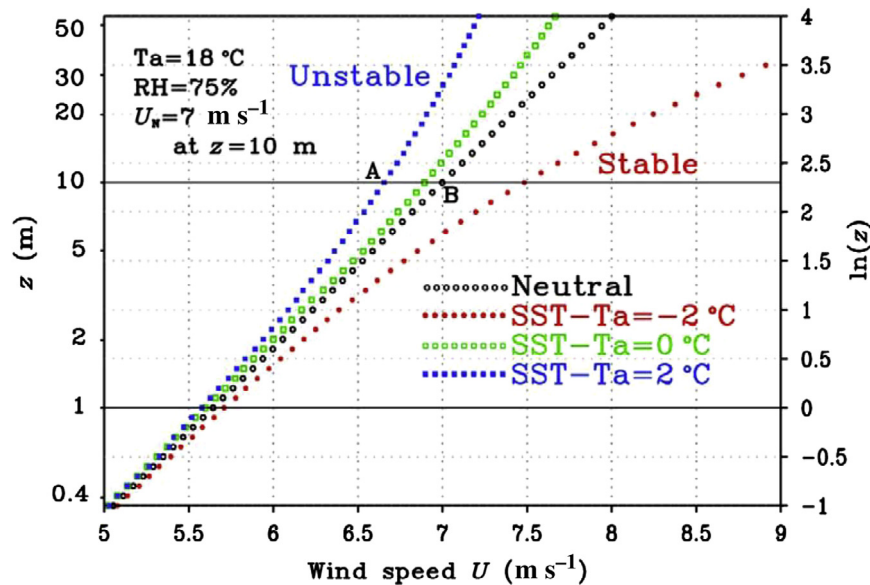


**Figure 6** Typical wind profiles at various stability conditions derived from the flux–profile relation by Liu et al. (1979). B is the equivalent neutral wind corresponding to the actual wind measurement at A.

to weak wind–stress variations but is more subjective toward atmospheric effects and rain contamination. Wind retrieval at the L-band (1 GHz) has also been attempted because L-band backscatter is not sensitive to atmosphere and rain attenuation. There have been calls for a multifrequency scatterometer that is sensitive to various parts of the ocean surface wave spectrum and may reduce atmospheric and rain effects.

Present scatterometers are real-aperture systems, and the spatial resolution is limited by the antenna size. A larger antenna will, of course, enhance the spatial resolution. Another way to achieve higher resolution is to add synthetic aperture capability.

One of the drawbacks of present scatterometers is the ambiguity in retrieving wind–stress direction. The backscatter is a cosine function of the azimuth angle. In a recent experiment, it was demonstrated that the correlation between copolarized and cross-polarized backscatter of radiance is a sine function of the azimuth angle. By adding polarized measurement capabilities to the scatterometer, the directional ambiguity problem could be mitigated.

One polar-orbiting scatterometer at a low-altitude (e.g., 800 km) orbit can sample at a location on Earth not more than two times a day. Additional instrument flying in tandem will allow descriptions of higher temporal variability and the reduction of the aliasing (bias introduced by subsampling) of the mean wind–stress.

Not all space-based ocean surface wind and stress measurements are comparable in quality. Standardizing the technology requirements for observation accuracy with different research and operational applications and for international cooperation is very desirable. Many scientific reports have affirmed the need for high-quality, continuous, and consistent long time series of ocean surface vector winds and stress.

## Acknowledgment

This article was prepared at the Jet Propulsion Laboratory, California Institute of Technology, under contract with the National Aeronautics and Space Administration (NASA). It was supported by the Ocean Vector Winds and the Physical Oceanography Programs of NASA. Xiaosu Xie and Wenqing Tang provided valuable assistance.

**See also:** Air Sea Interactions: Momentum, Heat, and Vapor Fluxes. **Boundary Layer (Atmospheric) and Air Pollution:** Surface Layer.

## Further Reading

- Barale, V., Gower, J.F.R., Alberolanza, L., 2010. *Oceanography from Space*. Springer, Dordrecht. pp. 93–111 (Chapter 6).
- Emanuel, K., 1995. Sensitivity of tropical cyclones to surface exchange coefficients and a revised steady state model incorporating eye dynamics. *Journal of the Atmospheric Sciences* 52, 3969–3976.
- Gower, J., 2006. *Remote Sensing of the Marine Environment, Manual of Remote Sensing*, third ed. vol. 6. American Society for Photogrammetry and Remote Sensing. pp. 149–178 (Chapter 5).
- Liu, W.T., Katsaros, K.B., Businger, J.A., 1979. Bulk parameterization of air–sea exchanges in heat and water vapor including the molecular constraints at the interface. *Journal of the Atmospheric Sciences* 36, 1722–1735.
- Liu, W.T., Xie, X., Niiler, P.P., 2007. Ocean–atmosphere interaction over Agulhas extension meanders. *Journal of Climate* 20, 5784–5797.
- Muyeen, S.M., 2010. *Wind Energy Conversion Systems*. Springer-Verlag, London. pp. 367–383 (Chapter 15).